The past history of galaxy clusters told by their present neighbours

Jenny G. Sorce, Stefan Gottlöber, Gustavo Yepes

Monthly Notices
of the
ROYAL ASTRONOMICAL SOCIETY

MNRAS **496,** 5139–5148 (2020)
Advance Access publication 2020 July 7

doi:10.1093/mnras/staa1831

The past history of galaxy clusters told by their present neighbours

Jenny G. Sorce,[1,2,3]★ Stefan Gottlöber[3] and Gustavo Yepes[4,5]

[1]*Univ Lyon, ENS de Lyon, Univ Lyon1, CNRS, Centre de Recherche Astrophysique de Lyon UMR5574, F-69007 Lyon, France*
[2]*Univ Lyon, Univ Lyon1, ENS de Lyon, CNRS, Centre de Recherche Astrophysique de Lyon UMR5574, F-69230 Saint-Genis-Laval, France*
[3]*Leibniz-Institut für Astrophysik (AIP), An der Sternwarte 16, D-14482 Potsdam, Germany*
[4]*Departamento de Física Teórica, Universidad Autónoma de Madrid, Cantoblanco, E-28049 Madrid, Spain*
[5]*Centro de Investigación Avanzada en Física Fundamental, Facultad de Ciencias, Universidad Autónoma de Madrid, E-28049 Madrid, Spain*

Accepted 2020 June 11. Received 2020 June 9; in original form 2020 February 20

ABSTRACT

Galaxy clusters can play a key role in modern cosmology, provided their evolution is properly understood. However, observed clusters give us only a single timeframe of their dynamical state. Therefore, finding present observable data of clusters that are well correlated to their assembly history constitutes an inestimable tool for cosmology. Former studies correlating environmental descriptors of clusters to their formation history are dominated by halo mass–environment relations. This paper presents a mass-free correlation between the present neighbour distribution of cluster-size haloes and the latter mass assembly history. From the Big Multidark simulation, we extract two large samples of random haloes with masses ranging from Virgo to Coma cluster sizes. Additionally, to find the main environmental culprit for the formation history of the Virgo cluster, we compare the Virgo-size haloes to 200 Virgo-like haloes extracted from simulations that resemble the local Universe. The number of neighbours at different cluster-centric distances permits discriminating between clusters with different mass accretion histories. Similarly to Virgo-like haloes, clusters with numerous neighbours within a distance of about two times their virial radius experience a transition at $z \approx 1$ between an active period of mass accretion, relative to the mean, and a quiet history. In contrary, clusters with few neighbours share an opposite trend: from passive to active assembly histories. Additionally, clusters with massive companions within about four times their virial radius tend to have recent active merging histories. Therefore, the radial distribution of cluster neighbours provides invaluable insights into the past history of these objects.

Key words: galaxies: clusters: general – dark matter.

1 INTRODUCTION

Galaxy clusters are the largest virialized objects in the Universe. In the 1990s, they helped establishing the concept of a Universe with a matter density below the critical one (see Voit 2005) and they played a key role in the development of the current Lambda cold dark matter (ΛCDM) paradigm (see Allen, Evrard & Mantz 2011 for a review). The hierarchical model of structure formation, a key prediction of the ΛCDM model (e.g. Colberg et al. 1999; Evrard et al. 2002), can be tested precisely with measuring cluster abundances at different epochs. Observable quantities that are sensitive to the dark matter halo assembly history can thus contribute to our understanding of hierarchical structure formation. Any discrepancies between observations and theory may ultimately point towards necessary modifications of the model, including the nature of the dark matter particle or/and the properties of the initial density fluctuations (e.g. Komatsu et al. 2009). Galaxy clusters are thus standard tools for testing cosmological models.

However, their utility as probes depends grandly on the control of the various systematic uncertainties and on our understanding of the correlations between observable quantities and their mass.

In that respect, cluster structural features, like their fraction of substructures or their mass profile, largely correlated to their formation and evolution have been widely studied (e.g. Smith & Taylor 2008; Wong & Taylor 2012; Ludlow et al. 2013; Wu et al. 2013). The correlation between environment and assembly history has been much less investigated (see e.g. Faltenbacher et al. 2005). Only a few studies took an interest in studying potential relations between the large-scale environment (i.e. cosmic web) and the assembly history of galaxy clusters (e.g Foëx, Chon & Böhringer 2017; Musso et al. 2018, for both observational and theoretical studies). A few others focused on the small-scale environment but only briefly (Wong & Taylor 2012). In addition, Haas, Schaye & Jeeson-Daniel (2012) warn us that the term 'environment' is used for a variety of measures that are mostly related to the halo mass. These underlying relations affect the signal that could exist between the current small-scale environment of clusters and their assembly history.

With the advent of larger and larger volume dark-matter-only cosmological simulations (e.g. Angulo et al. 2012; Fosalba et al. 2015; Klypin et al. 2016) with high-enough mass resolution (see, e.g. Prada et al. 2016, Fig. 1 for a review), it becomes now possible to study the potential small scale–assembly history correlations for a large statistical sample of dark matter haloes within a restricted mass range, removing thus the mass dependence. This paper proposes such a study.

★ E-mail: jenny.sorce@ens-lyon.fr / jsorce@aip.de

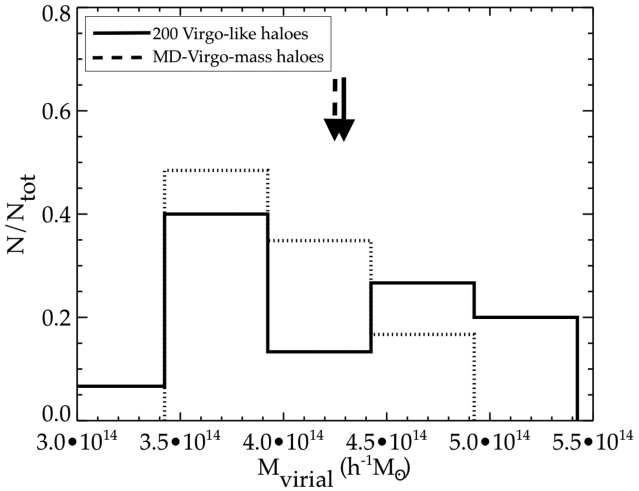

Figure 1. Mass distributions of the 20 226 dark matter haloes, selected in the MultiDark simulation to constitute the MD-Virgo-mass sample (dotted line) and of the 200 Virgo-like haloes of the constrained simulations (solid line). The arrows stand for the respective mean mass of the Virgo-like and the MD-Virgo-mass haloes.

Beyond looking for a correlation between the current environment of clusters and their accretion histories in general, this paper pursues also a second goal with identifying key properties of our local environment that are responsible for the history of Virgo, our closest cluster neighbour. Indeed in previous work, using simulations designed to resemble our local Universe,[1] we showed that the simulated Virgo-like clusters have had a quiet assembly history within the past seven gigayears while they were more active earlier on (Sorce et al. 2016a). Namely, while the Virgo-like clusters used to accrete lots of objects in their early stages of evolution, nowadays, they still do but to a much smaller extent. In a more recent study (Sorce, Blaizot & Dubois 2019) that enlarged our previous sample from 15 to 200 Virgo counterparts and increased their resolution by a factor of 3, we found that this kind of assembly history is rare and that this is most probably due to the local environment. This study compared the properties of more than 400 cluster-size random haloes to the 200 Virgo-like haloes. At $z = 0$, only 18 per cent of the random haloes have, besides a similar merging history from $z = 4$ to the end, mean radius, velocity dispersion, number of substructures, spin, velocity, concentration, and centre of mass offset with respect to the spherical centre within 3σ of Virgo-like halo properties. This correspondence reduces to 0.5 per cent at 2σ and zero at 1σ. These small rates are due to large-scale environmentally induced properties like the velocity. In addition, $z \approx 1$ appears like the redshift of change between the mean assembly history of the Virgo-like haloes and that of random haloes: From being more active in accreting mass on average than random haloes at $z > 1$, the Virgo-like haloes become quieter for $z < 1$. It is thus of great interest to understand which characterization of the cluster environment can be associated with such a specific assembly history.

To investigate this puzzle as well as more broadly potential small scale–assembly history correlations, one needs a large sample of random cluster-size haloes. The Big MultiDark simulation (BigMDPL), one of the largest computational volumes of the MultiDark simulation series using Planck cosmology (Klypin et al. 2016), provides us with such a sample. We extract from this large cosmological simulation two different cluster catalogues. One with ∼3000 cluster-size haloes with masses within (8–10) $\times$ 10^{14} h^{-1} $M_\odot$ and another set of more than 20 000 haloes within the mass range (3.7–5.0) $\times$ 10^{14} h^{-1} $M_\odot$. This second set matches our 200 Virgo-like sample with a mean mass of 4.3×10^{14} h^{-1} $M_\odot$ and a standard deviation of 0.66×10^{14} h^{-1} $M_\odot$. We then compare their evolution. As a consistency check, it is worth mentioning that Tully (2015) published a compilation of the virial masses of nearby clusters. Assuming Planck cosmology, the observational mass estimate of the Virgo cluster translates into $M_{\rm vir} \sim 4.7 \times 10^{14}$ h^{-1} $M_\odot$, in good agreement with the masses obtained for the Virgo-like haloes.

This paper starts in Section 2 with a brief description of our 200 Virgo-like haloes used as a gauge to determine our environmental property responsible for such an assembly history. Then, it introduces the BigMDPL simulation and describes at length the samples and subsamples of selected cluster-size random haloes used to determine the small scale–assembly history correlations. In Section 3, correlations between the assembly history of the cluster haloes and their current number of substructures as well as the present number, mass, and cluster-centric distance of their neighbours are sought for. In Section 4, we explore the impact of the presence/absence of massive neighbours on assembly histories to match that of Virgo-like haloes. Finally, Section 5 summarizes the main finding: A new correlation between the current neighbours of clusters and their accretion history is confirmed independently of their mass.

2 SIMULATIONS AND CLUSTER HALO (SUB)SAMPLES

For our two-goal study, two types of dark-matter-only simulations are required to build the cluster halo (sub)samples: (1) a set of constrained cosmological simulations resembling the local Universe that contain a realistic Virgo-like halo, and (2) a large-volume cosmological simulation that contains a statistically significant number of massive and Virgo-size cluster haloes. All these dark-matter-only simulations are based on the Planck cosmology ($H_0 = 67.77$ km s^{-1} Mpc^{-1}, $\Omega_\Lambda = 0.693$, $\Omega_{\rm m} = 0.307$, $\sigma_8 = 0.823$; Planck Collaboration XVI 2014).

2.1 Constrained simulations and Virgo-like haloes

We use 200 constrained simulations designed to match the large-scale structure around the Local Group within a ∼150 h^{-1} Mpc sphere radius. Local observational data used to constrain the initial conditions of the simulations are distances of galaxies and groups converted into peculiar velocities (Sorce et al. 2016b; Sorce & Tempel 2018) that are bias minimized (Sorce 2015). The details of the algorithms and steps to get the simulations are given in Sorce et al. (2019).

Built originally for the latter study, each one of the constrained simulations contains a Virgo-like halo at around the position of the observed Virgo cluster by analogy. To minimize the computing time, the zoom-in technique (Bertschinger 2001), implemented in the MUSIC code (Hahn & Abel 2011), was used to reach an effective resolution of 2048^3 particles in the full box (i.e. a dark matter particle mass of 1.2×10^9 h^{-1} $M_\odot$) within a 10 h^{-1} Mpc radius sphere centred on the Virgo-like haloes.

[1]The initial conditions of such simulations stem from the ΛCDM paradigm like any cosmological initial conditions based on this model. They also match a catalogue of local observational constraints to result in simulation with the local large scale structure, including Virgo-like haloes at $z = 0$, thanks to recent improvements.

Virgo-like halo properties and assembly histories were obtained with the AHF code combined to the MergerTree algorithm (Knollmann & Knebe 2009). Since, solely, the mass evolution of the Virgo haloes is used for comparison with the large sample of dark matters haloes in this paper and since this evolution depends only on the cosmological model, the chosen halo finder method used to derive this mass evolution is not critical.

These 200 simulated counterparts of the Virgo cluster constitute our first halo sample:

(i) 200 Virgo-like: These haloes match the observations extremely well and share similar properties, including the assembly history. Namely, the cosmic variance is effectively reduced down to the cluster scale (Sorce et al. 2016a; Sorce 2018; Olchanski & Sorce 2018; Sorce et al. 2019). The latter investigation of these simulations led to the current search for the environmental properties responsible for the specificities of the Virgo cluster assembly history.

2.2 Cluster haloes in the MultiDark simulation

Cluster haloes are taken from the BigMDPL simulation, which is part of the MultiDark simulation series (Klypin et al. 2016). It is the second largest boxsize of this series to have been run.[2] With 2.5 Gpc h^{-1} as a side and 3840^3 particles, it has a mass resolution of $2.4\times10^{10}\,h^{-1}\,M_\odot$. This simulation has been run with the same cosmological parameters as the constrained simulations.

Halo and subhalo catalogues at different redshifts were extracted from the simulation using the ROCKSTAR algorithm (Behroozi, Wechsler & Wu 2013a). Although all subsequent conclusions are identical when using all haloes and subhaloes with more than 50 or 100 particles, to be more conservative, we retain only (sub)haloes with more than a hundred particles. The merger trees were obtained from the ROCKSTAR catalogues using the CONSISTENT TREES software (Behroozi et al. 2013b). From this simulation at $z = 0$, we extracted two samples of distinct cluster-size haloes that are not substructures of more massive parent haloes:

(i) MD-massive: a sample of massive clusters with masses in the range $(8–10)\times10^{14}\ h^{-1}\ M_\odot$, which contains 2682 objects at redshift zero.

(ii) MD-Virgo-mass: a sample of Virgo-size haloes selected to be within the same mass range as the sample of constrained Virgo-like haloes that is described in Section 2.1. More precisely, a halo is retained for further study if its mass is within 1σ of the mean mass of the Virgo-like haloes, where σ^2 is the mass variance of the Virgo-like halo sample. This second sample contains 20 226 objects. Fig. 1 shows their mass distribution as well as that of the Virgo-like haloes.

2.3 Subsamples and deviation from mean assembly history

Among the three considered subsamples, only the 200 Virgo-like haloes share similar environment and assembly history by construction. Instead, the clusters in the MD-massive (respectively, MD-Virgo-mass) samples share only the same mass.

As a case in point, Fig. 2 shows the mean mass assembly history as a function of look-back time (lower axis) or redshift (upper axis) of 200 Virgo-like (solid orange line) and MD-Virgo-mass (blue dotted line) samples. The coloured areas depict their respective standard deviation. As it is clearly shown, the 200 Virgo-haloes do not follow the mean of the MD-Virgo-mass haloes. In fact, during the last few

[2]https://www.cosmosim.org/cms/simulations/bigmdpl/.

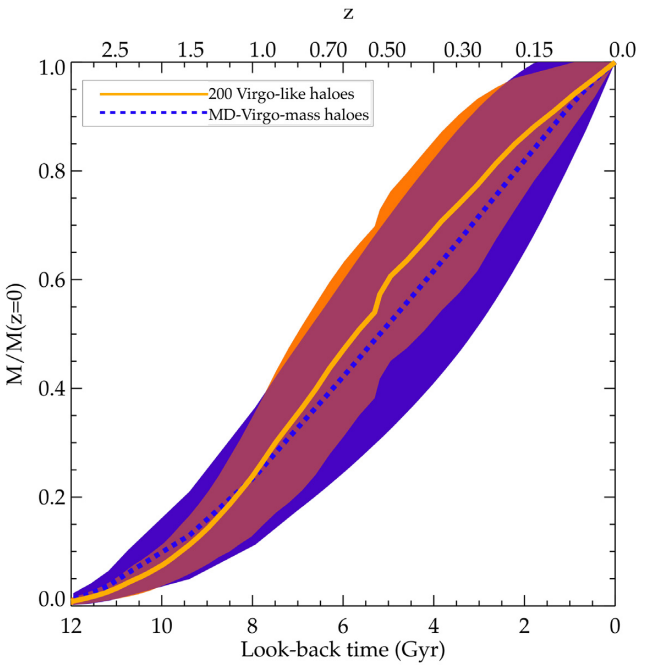

Figure 2. Mean mass assembly history of the MD-Virgo-mass (blue dotted line) and the 200 Virgo-like (orange solid line) samples. Shaded areas give the standard deviations.

gigayears, the Virgo-haloes had a quieter assembly history than the mean of the random cluster haloes. Our previous papers already demonstrated this result, although based on much smaller random halo samples (Sorce et al. 2016a, 2019). Additionally, it is remarkable that despite the much smaller number of haloes in the Virgo sample, the scatter of the assembly history of 200 Virgo-like haloes is smaller than that of the MD-Virgo-mass sample. This is due to the constrained nature of the simulations.

Fig. 2 represents also the starting point of our search for a correlation between environment and mass accretion history. It is indeed striking that constraints set by the observed velocity field of galaxies in a large volume around the Local Group lead to the prediction of a specific mass assembly history for the Virgo cluster. It is thus interesting to find out whether a subsample of the MD-Virgo-mass haloes based on similar environmental properties has an assembly history matching that of the 200 constrained Virgo-like haloes.

The present numbers of substructures and neighbours are two observable quantities in clusters. Subsequently, we divide the halo samples into subsamples according to their number of either substructures or neighbours at $z = 0$ following Table 1 (each subsample range is specified in the tables of Appendix A). The number of substructures/neighbours *per se* is not meaningful: It depends on the resolution of the simulation (i.e. the smallest substructure/neighbour that can be identified) and on the halo finder used. In addition, it is difficult to compare the observed (Boselli et al. 2014) and the predicted numbers because of projection effects and mass estimate uncertainties in observations especially for substructures. Consequently, to be able to apply this study both to simulations and observations, we split the MD-massive and MD-Virgo-mass samples into different subsamples using the mean number of substructures/neighbours ($\overline{n}$) above a given mass and its standard deviation (σ_n) as references.

Subsequently, cluster haloes can then be categorized from those with no or very few substructures/neighbours up to haloes with

Table 1. Definition of the different halo subsamples based on their number n of substructures and neighbours.

Sample	Line type	Colour of lines and areas
$n < \overline{n} - 2\sigma_n$	Dotted	Black line (dark violet)
$\overline{n} - 2\sigma_n < n < \overline{n} - \sigma_n$	Short dashed	Violet line (light violet)
$\overline{n} - \sigma_n < n < \overline{n}$	Dash–dotted	Blue (light blue)
$\overline{n} < n < \overline{n} + \sigma_n$	Dash–three-dotted	Blue-green (Light blue-green)
$\overline{n} + \sigma_n < n < \overline{n} + 2\sigma_n$	Long dashed	Orange (light orange)
$n > \overline{n} + 2\sigma_n$	Dotted	Red (light red)

Note. The line types and the coloured regions refer to Figs 3–5.

a large number of substructures/neighbours going through intermediate numbers. The main goal of this paper is to find a new probe that can be used in observational studies. The observational counterparts of simulated dark matter substructures are the galaxies and subgroups of a cluster that are grandly affected by project effects. Therefore, using substructures for our analyses, while interesting, will not be particularly usable in observations. Observationally, cluster neighbours are more easily identified and characterized than substructures. Thus, we go further by introducing neighbour cluster centric distances and masses in the subsample selection criteria. This can be done similarly in all the simulated and/or observed samples. Furthermore, this process should permit classifying observed clusters into the above categories even in the case of random and/or systematic biases applying to the whole observational sample provided that the latter is statistically significant (i.e. with significant mean and standard deviation). Appendix A gives the number of haloes per subsample as well as the different ranges for the number of substructures/neighbours.

In order to find possible correlations between the assembly history of clusters and their *current* cluster properties, like the number of substructures or the number, mass, and cluster-centric distances of neighbours, we then compare the mean assembly histories of the haloes in the different subsamples with the mean merger history of the total samples and of the constrained Virgo haloes for the MD-Virgo-mass sample. To that end, we define the ratio $Q(t)$ as follows:

$$Q(t) = \frac{\frac{1}{N_c}\sum_{j=1}^{N_c} M_{j,\,\mathrm{virial}}(t)/M_{j,\,\mathrm{virial}}(0)}{\frac{1}{N}\sum_{i=1}^{N} M_{i,\,\mathrm{virial}}(t)/M_{i,\,\mathrm{virial}}(0)}, \quad (1)$$

where N is the total number of cluster haloes and N_c is the number of cluster haloes that match a given criterion c in either MD-Virgo-mass or MD-massive. $M_{i,\,\mathrm{virial}}(t)$ is the virial mass of the halo i at look-back time t and today $t = 0$.

In other words, the quantity Q is the ratio of mean assembly histories or the deviation from the mean assembly history at a given time. Any deviation from the unity means that the haloes selected under the criterion c have on average a history that deviates from the mean. If $Q(t) > 1$ at a given time, the selected haloes are quieter than on average. They already grew in the past to reach their mass value at present. Reversely, if $Q(t) < 1$, the selected haloes are, at that time, more active than that on average since they need to grow faster to reach their mass today.

3 ASSEMBLY HISTORY

Rather than focusing on the formation time of galaxy clusters like in previous studies (e.g. Wong & Taylor 2012), analyses in this paper are directed towards the type of accretion history: passive, active, quiet, or a combination of these across cosmic time. These adjectives are used to describe the mass evolution or growth of the haloes. A fast growth is associated to an active assembly history while a slow increase in mass is due to a quiet or even passive history in case of quasi- or even absence of matter accretion.

3.1 Number of substructures

The number of substructures of a halo is defined as the number of subhaloes within its virial radius. The virial radius of a halo is defined as the radius of a sphere whose density is $\Delta_{\mathrm{vir}}(z) \times \Omega_{\mathrm{m}}\rho_{\mathrm{c}}$ at that redshift. $\Delta_{\mathrm{vir}}(z)$ is given by the spherical collapse model in a given cosmology. In ROCKSTAR, this value is taken from the analytical fitting formula given in Bryan & Norman (1998).

Fig. 3 presents $Q(t)$: the different mean assembly histories of halo subsamples relative to the total mean history of the MD-Virgo-mass and MD-massive samples, respectively. As expected, clusters with the largest number of substructures (more massive than $2.5\times10^{12}\,h^{-1}\,\mathrm{M}_\odot$, left-hand panels, or more massive than $2.5\times10^{13}\,h^{-1}\,\mathrm{M}_\odot$, right-hand panels) have had, on average, the most active assembly histories ($Q(t) < 1$, warmest colours) while those with a few substructures have had, on average, the most passive histories ($Q(t) > 1$, coldest colours). Within the last few gigayears, the former grows faster than the average while the latter grows slower. Light coloured areas stand for standard deviations of the mean curves. The different scenarios are quite distinguishable, confirming the link between the current number of substructures and the assembly history of galaxy clusters already reported by e.g. Sereno & Zitrin (2012).

However, none of the subsamples built from the MD-Virgo-mass sample presents a change of trend at $z \approx 1$ like that observed for the Virgo-like haloes (solid green line). In other words, no average line crosses the ordinate equals to 1 line at $z \approx 1$, which would indicate that this subsample contains haloes that used to grow faster than on average at $z > 1$ and that later grow slower than on average. This means that Virgo-like haloes cannot be identified solely by the number of substructures they have at present. This is quite expected: While the Virgo haloes have had a quiet assembly history within the past few gigayears, they have a larger, rather than a smaller, total number of substructures than random haloes on average (Sorce et al. 2019). The number of substructures is therefore not sufficient to identify haloes with a assembly history similar to that of Virgo-like haloes. Therefore, in the next section, we explore this issue in more detail and focus on the abundance, masses, and cluster-centric distances of cluster neighbours at present.

3.2 Number and clustercentric distance of neighbours

In this section, the cluster halo samples are split into six subsamples according to the number of neighbours within a given distance (from the virial radius of the cluster haloes to either $\sim$2, $\sim$4, or $\sim 8r_{\mathrm{vir}}$) and with a given minimum mass (either 2.5×10^{12} or $2.5\times10^{13}\,h^{-1}\,\mathrm{M}_\odot$). In Fig. 4, the ratio $Q(t)$ (equation 1) is shown for the different subsamples of both the MD-Virgo-mass (top panels) and MD massive (bottom panels) samples. As in the previous figure, standard deviations are shown as light coloured areas. In the top six panels, the solid green line stands for the average assembly history of the 200 Virgo-like haloes divided by the mean assembly history

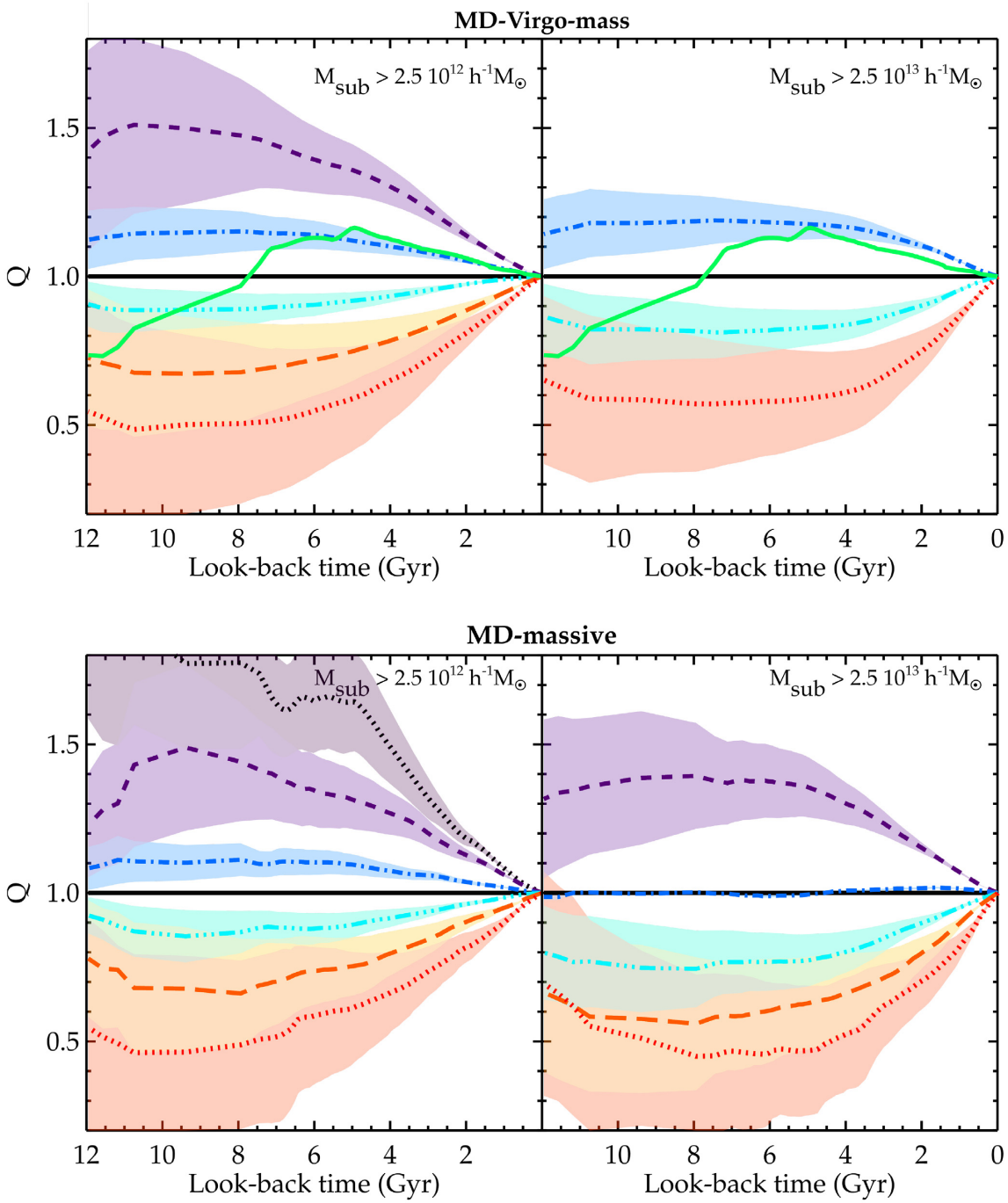

Figure 3. Q ratios for the MD-Virgo-mass (top panels) and MD-massive (bottom panels) samples. Left-hand (right-hand) panels are limited to substructures with masses $M_{\rm sub}$ greater than $2.5\times10^{12}\,h^{-1}$ M$_\odot$ ($2.5\times10^{13}\,h^{-1}$ M$_\odot$). Different coloured lines (Table 1) show the trend of subsamples built on the basis of the number of substructures, which is increasing from the black dotted line to the red dotted line (see Table A1). Coloured areas give the standard deviations. The solid green lines in the top panels stand for the ratio Q obtained for the 200 Virgo-like haloes with respect to the MD-Virgo-mass sample.

of all the haloes in MD-Virgo-mass. Findings as described below are here again quite similar for both mass ranges.

According to Fig. 4, the various cluster subsamples exhibit quite different behaviors, although these behaviors are similar between haloes of the two mass ranges. The main results drawn from this figure are summarized as follows:

(i) Left-hand panels of the first and third rows: Assembly histories are alternatively quiet or active, i.e. $Q(t) - 1$ changes sign over time. The sought for behaviour with a redshift of change appears distinctly. The transition redshift ($z \approx 0.7$ or $t \approx 6$ Gyr) is close to that observed for the Virgo-like haloes ($z \approx 1.0$ or $t \approx 8$ Gyr). Namely, after that redshift, haloes with currently many neighbours (dotted and long-dashed lines, warmest colours) had a passive assembly history ($Q > 1$), while before $z = 0.8$, they tended to have had an active assembly history ($Q < 1$). The reverse is true for haloes with presently only a few neighbours (coldest colours). Note that for the most massive haloes with the largest number of neighbours (left-hand panel of

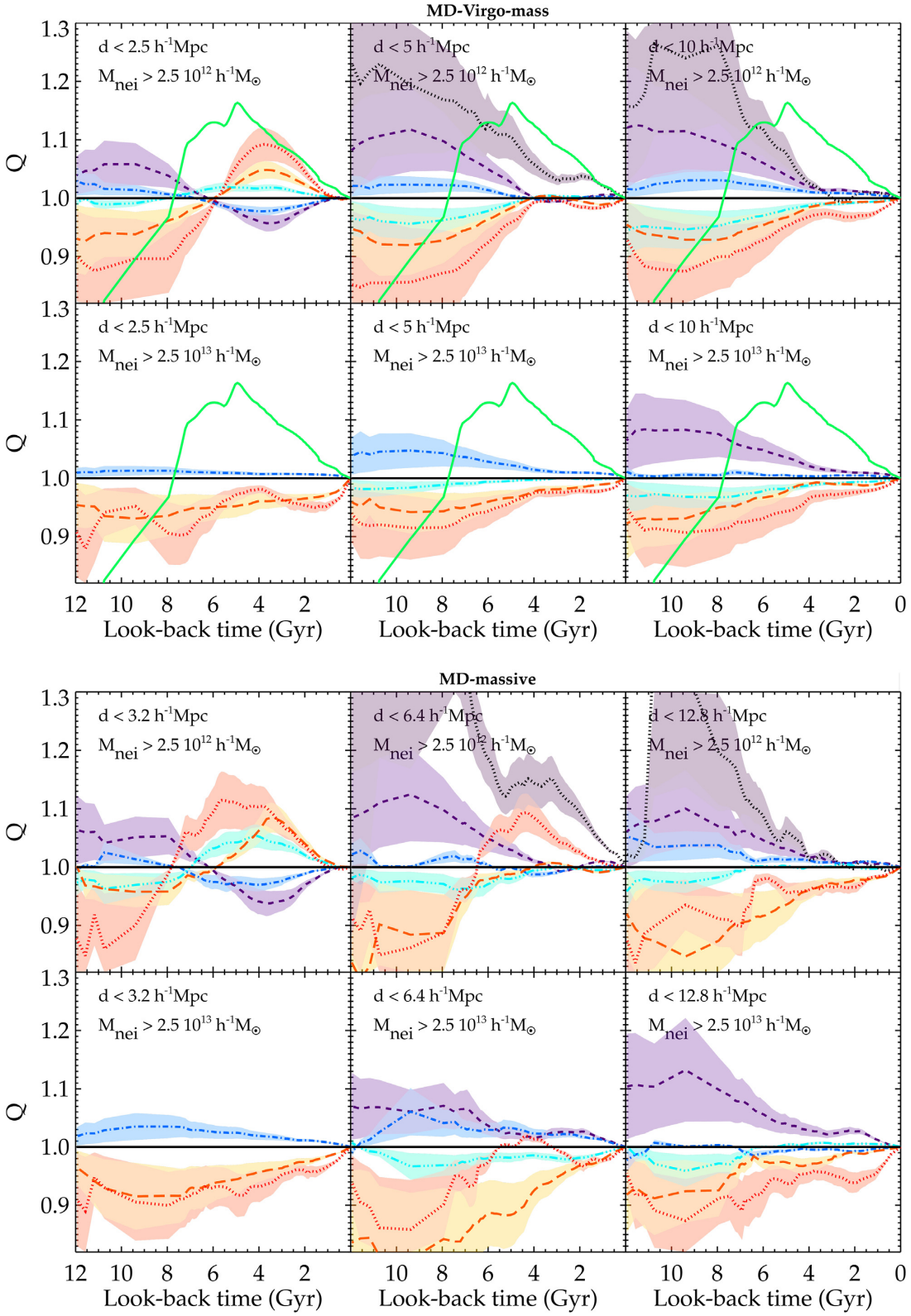

Figure 4. Q ratios for the MD-Virgo-mass (top six panels) and MD-massive (bottom six panels) samples. First and third (second and fourth) row panels account for neighbours more massive than $2.5\times10^{12}\ h^{-1}\ \mathrm{M}_{\odot}$ ($2.5\times10^{13}\ h^{-1}\ \mathrm{M}_{\odot}$). From left to right, more and more distant (within $\sim$2, $\sim$4, and $\sim8r_{\mathrm{vir}}$) neighbours are included in the count. Different coloured lines (Table 1) show the trend of subsamples built on the basis of the present number of neighbours, which is increasing from the black dotted line to the red dotted line (see Table A2). Coloured areas give the standard deviations. The solid green lines in the two first rows of panels stand for the ratio Q obtained for the 200 Virgo-like haloes with respect to the MD-Virgo-mass sample.

the third row), their redshift of change is even closer to that of the 200 Virgo-like haloes. This is probably due to the smaller number of haloes in that subsample with respect to 10 times more haloes in the other subsamples, with the 200 Virgo-like halo sample having an intermediate number. Indeed, the smoother the trends, the more populated are the subsamples. It flattens the curves and gives an average intermediate redshift of change of $z \approx 0.7$. Note that the absence/presence of a massive neighbour is responsible for this shift in the redshift of change. As we will show below, a massive neighbour contributes to maintaining an accretion activity, and thus shifts the change of behaviour to later times while its absence permits an earlier change. To summarize, independently of their mass, haloes with currently the largest number of neighbours (dotted line) in a very close vicinity (less than $\sim 2r_{\rm vir}$) entered the quieter assembly history ($Q > 1$) mode more recently.

(ii) Middle panels of the first and third rows: Transition signals are clearly dampened with the exception of the most massive haloes with the largest number of neighbours. There are small ripples recently, but it is harder to discriminate between the assembly histories of haloes when including their more distant neighbours.

(iii) Right-hand panels of the first and third rows: The above-mentioned trend is confirmed. The assembly histories of the different subsamples are mostly quiet or active at all times. Namely, when including neighbours within 10–12 h^{-1} Mpc, the transition disappears. It makes it more challenging to discriminate the recent assembly histories of haloes. This is most probably due to both the increasing probability of encountering more and more massive neighbours with the distance from the clusters and the limit of the 'small scale'/cluster interaction.

(iv) Left-hand panels of the second and fourth rows: Indeed, when considering only massive neighbours, the redshift of transition does not appear anymore. Haloes with the largest number of close-by massive neighbours (dotted line) tend to be more active ($Q < 1$) than whose without even at late times. These massive neighbours do not permit discriminating as efficiently as the small neighbours do between halo recent assembly histories.

(v) Middle and right-hand panels of the second and fourth rows : Again the existence of neighbours more massive than $2.5 \times 10^{13}\, h^{-1}\, {\rm M}_{\odot}$, i.e. 1–3 per cent of the main halo mass, prevents a change of the assembly history irrespective of their distance, i.e. an active/quiet assembly history remains, on average, active/quiet. The massive neighbours of a halo contribute to its gravitational potential and thus support its active history.

To summarize, small neighbour counts in the close vicinity permit discriminating the recent assembly history of haloes. Massive neighbours help haloes accreting mass. Thus, they maintain their accretion activity, most probably resulting in a shift of their redshift of change to later times. However, when considering neighbours at larger distances, the signal is dramatically damped. Therefore, there exists a well-established correlation between the current number of close-by small neighbours of a cluster-size halo and its past assembly history that can be further refined when considering the presence or absence of massive neighbours.

4 MASSIVE NEIGHBOURS DRIVE THE REDSHIFT OF CHANGE

To go deeper into refining our correlation and identifying the type of neighbours required to get a Virgo-like assembly history, it is worth emphasizing yet again that the change of sign of $(Q(t) - 1)$ becomes weaker from the left- to right-hand side in the top panels of Fig. 4. When including more distant neighbours, the signal is damped because of the increasing probability of encountering heavier neighbours than within shorter distances. Since Virgo is known not to have (numerous) massive neighbours within 5 h^{-1} Mpc and actually no neighbour of the same order of mass, it is interesting to further reduce our full sample of random haloes within the same mass range as Virgo haloes by excluding those that have massive neighbours in their vicinity.

To this end, we redefined the ratio $Q(t)$ in equation (1), to hereafter $Q^{'}(t)$, assuming now that the denominator is summed over a sample of cluster haloes, excluding those with neighbours more massive than $10^{13}\, h^{-1}\, {\rm M}_{\odot}$ within 2.5 and 5 h^{-1} Mpc. This reduces the total number of cluster haloes in MD-Virgo-mass to 13 285 and 3108, respectively.

Fig. 5 is thus similar to Fig. 4 but restricted to haloes without neighbours more massive than $10^{13}\, h^{-1}\, {\rm M}_{\odot}$ within a 2.5 and 5 h^{-1} Mpc radius (from the left- to right-hand side). The left-hand panel shows the best agreement with the mean assembly history of the Virgo counterparts during the last 4 gigayears. The redshift of change is even now shifted to earlier times (from 6 to 7 Gyr, corresponding to a shift from $z \approx 0.7$ to ≈ 0.8). Note that our sharp limits in distances and masses have a small influence on the results. Typically, allowing a few neighbours slightly above $10^{13}\, h^{-1}\, {\rm M}_{\odot}$ within 5 h^{-1} Mpc does not make a significant difference. We performed several tests to confirm that our conclusions are rather independent on the exact maximum mass value chosen to count neighbours.

The fact that the Virgo cluster does not have a nearby massive neighbour, combined with the multitude of leftover small neighbours, explains its quiet assembly history nowadays as well as its redshift of change. This multitude of close-by small neighbours suggests also that it had an active assembly history in the past. It used to have a strong accretion rate but it slowed down lately. Thus, a multitude of small neighbours are still in its vicinity. They are approaching but have not been accreted yet. The environment has not been 'wiped' out by accretion unlike for the haloes with very few small neighbours: haloes that used to be passive and are now active. These haloes did not grow in the past (passive history) and, thus, to reach the mean mass of our Virgo sample, they need to accrete mass faster nowadays. This is reinforced by the absence of a massive neighbour that would otherwise maintain its strong accretion rate.

Consequently, we identify the relative number of current neighbours, within $\sim$2.5–5 h^{-1} Mpc (two to four times the virial radius), with masses at least about two orders of magnitude below the mass of the cluster, as the important parameter to determine whether the past assembly history of a Virgo-size halo was more active before and quieter after the redshift of change compared to the average merging history of a large sample of clusters. Observational effects could systematically bias the number of neighbours. This is not critical, since this number is not relevant *per se*. This number of neighbours must be compared to the average number of neighbours of the cluster sample. Note that this relation holds for more massive haloes.

A second parameter permits refining more precisely the past history (i.e. the redshift of change): the presence or absence of large neighbours (at least above about 2 per cent the mass of the cluster) within the same radius. A large neighbour indeed nurtures an active accretion history.

This study shows that the Virgo cluster, which has had a quiet assembly history recently while being more active in the past, has an assembly history similar to that of dark matter haloes within the same mass range, without massive companion within 2.5 h^{-1} Mpc,

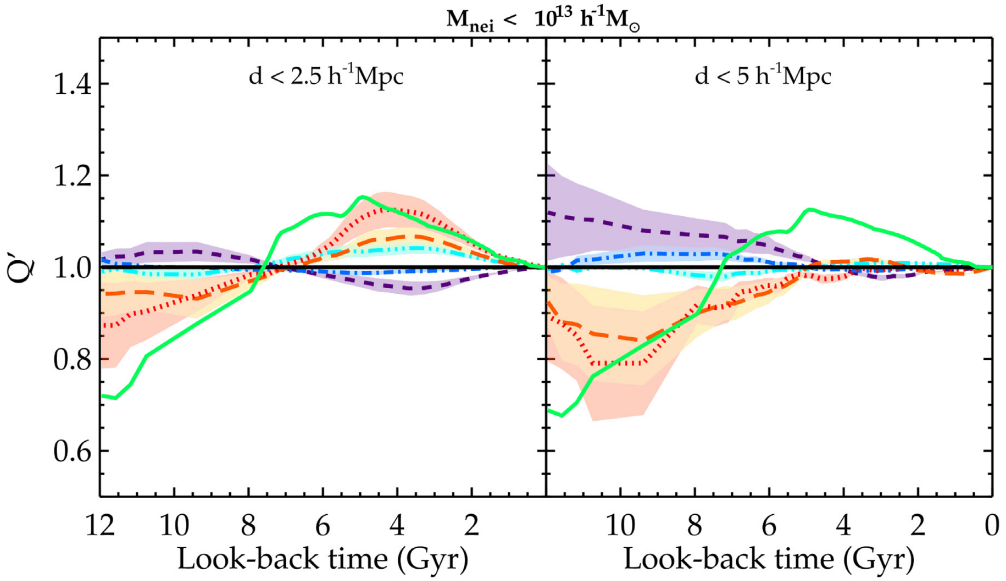

Figure 5. Same as the two first panels of Fig. 4 but for a restricted sample of dark matter haloes within MD-Virgo-mass: Only haloes with no neighbours more massive than 10^{13} h^{-1} $M_\odot$ within 2.5 and 5 h^{-1} Mpc radii (from the left- to right-hand side) are retained. Different coloured lines (Table 1) show the trend of subsamples built on the basis of the present number of neighbours, which is increasing from the black dotted line to the red dotted line (see Table A3). Coloured areas give the standard deviations. The solid green lines stand for the ratio Q obtained for the 200 Virgo-like haloes with respect to the MD-Virgo-mass restricted sample.

but with a multitude of small neighbours within the same radius. Reversely, haloes within the same mass range ,without massive companions but with very few small neighbours within 2.5 h^{-1} Mpc, have had an active assembly history within the last gigayears and used to be more passive in the past, in the sense that their mass used to evolve slower than an average halo.

Moreover, only 473 out of 20 226 haloes present, on average, a history similar to Virgo, confirming that clusters like our closest neighbour are quite rare. In other words, 13 285 haloes of the total sample of 20 226 cluster haloes within a 2.5 h^{-1} Gpc cubic volume have no massive companion within 2.5 h^{-1} Mpc, and only 473 over 20 226 (2.3 per cent) have a multitude of small neighbours. They have, on average, an assembly history in agreement with that of the Virgo-like cluster lately (see Fig. 5, left-hand panel). Only a small fraction of haloes share the current environmental properties that imply that they had a similar assembly history as the Virgo-like cluster. A detailed study of these haloes with no massive neighbour within 2.5 h^{-1} Mpc and lots of small neighbours confirms that they all had a very similar assembly history. Differences are visible only before the redshift of change. In any case, they present the same trend and the variance is smaller than that for all the random haloes. We also notice the small variance in terms of the number of small neighbours as a function of the distance from the cluster centre. The variance value is at most similar to the variance of the entire sample despite the much higher number of haloes in the complete sample than in the selected subsample.

The number of current neighbours alongside their mass constitutes thus an alternative to the assembly history-type criterion required to select clusters similar to the Virgo cluster in addition to the mass and velocity selection criteria determined in Sorce et al. (2019).

5 CONCLUSION

Provided that they are well understood, galaxy clusters are standard tools for testing cosmological models like the hierarchical structure formation of ΛCDM. Observable quantities that are sensitive to the cluster assembly history constitute thus an inestimable knowledge to compare observed measurements to theoretical expectations.

This paper is mainly focused on finding a mass-free correlation between the relative number of current neighbours of cluster-size dark matter haloes and their mass assembly history. An underlying additional goal consists in uncovering properties of our environment responsible for the distinctive merging history of our closest cluster neighbour, the Virgo cluster.[3] Indeed, in previous studies based on Virgo-like clusters in the proper large-scale environment of constrained simulations, we found that Virgo-like haloes have had an active merging history in the past (before $z \approx 1$) while they are quieter nowadays (after $z \approx 1$) with respect to random haloes within the same mass range.

To achieve both our goals, we extract from the 2.5 h^{-1} Gpc boxsize MultiDark cosmological simulation two cluster-size halo samples. The first sample gathers all the haloes with masses ranging from 8×10^{14} to 10^{15} h^{-1} $M_\odot$ for a total of about 3000 haloes. The second sample is built with haloes within the same mass range (within 1σ) as our Virgo-like haloes for a total of more than 20 00 haloes.

These large cluster halo samples permit constructing subsamples based on several criteria, in particular with constraints on the current number and masses of neighbours of the cluster haloes. Trends arise independently of the halo sample/mass range considered. In fact, haloes with currently the largest number of neighbours in their close vicinity have a quieter assembly history recently than on average, while they used to be more active before $z \approx 1$. These haloes indeed did not accrete recently the neighbours in their vicinity

[3]Assuming a correlation between the assembly history of clusters and their environment, i.e. haloes sharing the same assembly history as the Virgo-like cluster should indeed live in the same environment.

and thus did not empty their close-by environment. In contrast, a low number of neighbours in this distance range is linked to the opposite assembly history: recently active and quieter in the past. Finally, massive companions (mass above about 2 per cent that of cluster haloes) within 2–4$r_{\rm vir}$ foster recent active assembly histories.

The most important parameter to determine the past assembly history of a cluster is thus the relative number of current neighbours with masses approximately two orders of magnitude below the mass of the cluster and within 1–4$r_{\rm vir}$.

Additionally, determining the presence or absence of massive neighbours (more massive than about 1/10th the mass of the cluster) within the same range of distances permits refining the selection of haloes matching the past history of Virgo-like. If there is no such massive neighbour within 2.5 h^{-1} Mpc, the assembly histories of the Virgo-like clusters and of the corresponding subsample of cluster haloes agree quite well over the most recent cosmic time. A comparison between the small number of haloes in the relevant subsamples to those of the large cluster halo sample confirms that the mass assembly history of the Virgo-like cluster (and therefore the Virgo cluster) is rare among all the possible merging histories. About 65 per cent of the total sample of cluster haloes have lots of small neighbours within short distances and less than 4 per cent have, in addition, no companion more massive than about 2–3 per cent of their mass.

To conclude, this study confirms that there exists a strong correlation between the current number of neighbours and the assembly history of clusters independently of the cluster mass. Eventually, it means that the environmental knowledge gives an alternative to the assembly history-type criterion required to select clusters similar to the Virgo cluster, a criterion to be added to the mass and velocity selection criteria given in Sorce et al. (2019). Because this correlation is based on relative rather than exact numbers of neighbours, it is expected to hold for both higher resolution and hydrodynamical simulations. Indeed, the higher resolution simulations will at most permit perhaps pushing the discrimination to higher redshifts by refining subsamples using smaller neighbour masses. Results based on already fully resolved neighbours will however not be affected. As for the hydrodynamical simulations, while the exact number of neighbours might be affected, there is no reason for the relative number to change because the exact numbers will be modified in the same way. This correlation is thus a priori valid for observations.

ACKNOWLEDGEMENTS

We would like to thank the referee for their very useful comments that helped clarify this paper. GY acknowledges financial support from MINECO/FEDER under research grant AYA2015-63810-P and MICIU/FEDER PGC2018-094975-C21. The authors would like to thank Adi Nusser for very useful discussions and suggestions. The authors gratefully acknowledge the Gauss Centre for Supercomputing eV (www.gauss-centre.eu) for funding this project by providing computing time on the GCS Supercomputer SuperMUC at Leibniz Supercomputing Centre (www.lrz.de). The ROCKSTAR catalogues and trees are available at the CosmoSim data base (www.cosmosim.org), which is a service by the Leibniz-Institute for Astrophysics Potsdam (AIP).

DATA AVAILABILITY

Two types of simulations are used in this paper. All the data regarding the random simulation are available at https://www.cosmosim.org/cms/simulations/bigmdpl/. As for the information regarding the Virgo cluster from constrained simulations, they are available upon request to the authors.

REFERENCES

Allen S. W., Evrard A. E., Mantz A. B., 2011, ARA&A, 49, 409
Angulo R. E., Springel V., White S. D. M., Jenkins A., Baugh C. M., Frenk C. S., 2012, MNRAS, 426, 2046
Behroozi P. S., Wechsler R. H., Wu H.-Y., 2013a, ApJ, 762, 109
Behroozi P. S., Wechsler R. H., Wu H.-Y., Busha M. T., Klypin A. A., Primack J. R., 2013b, ApJ, 763, 18
Bertschinger E., 2001, ApJS, 137, 1
Boselli A. et al., 2014, A&A, 570, A69
Bryan G. L., Norman M. L., 1998, ApJ, 495, 80
Colberg J. M., White S. D. M., Jenkins A., Pearce F. R., 1999, MNRAS, 308, 593
Evrard A. E. et al., 2002, ApJ, 573, 7
Faltenbacher A., Allgood B., Gottlöber S., Yepes G., Hoffman Y., 2005, MNRAS, 362, 1099
Foëx G., Chon G., Böhringer H., 2017, A&A, 601, A145
Fosalba P., Crocce M., Gaztañaga E., Castander F. J., 2015, MNRAS, 448, 2987
Haas M. R., Schaye J., Jeeson-Daniel A., 2012, MNRAS, 419, 2133
Hahn O., Abel T., 2011, MNRAS, 415, 2101
Klypin A., Yepes G., Gottlöber S., Prada F., Heß S., 2016, MNRAS, 457, 4340
Knollmann S. R., Knebe A., 2009, ApJS, 182, 608
Komatsu E. et al., 2009, ApJS, 180, 330
Ludlow A. D. et al., 2013, MNRAS, 432, 1103
Musso M., Cadiou C., Pichon C., Codis S., Kraljic K., Dubois Y., 2018, MNRAS, 476, 4877
Olchanski M., Sorce J. G., 2018, A&A, 614, A102
Planck CollaborationXVI, 2014, A&A, 571, A16
Prada F., Scóccola C. G., Chuang C.-H., Yepes G., Klypin A. A., Kitaura F.-S., Gottlöber S., Zhao C., 2016, MNRAS, 458, 613
Sereno M., Zitrin A., 2012, MNRAS, 419, 3280
Smith G. P., Taylor J. E., 2008, ApJ, 682, L73
Sorce J. G., 2015, MNRAS, 450, 2644
Sorce J. G., Gottlöber S., Hoffman Y., Yepes G., 2016a, MNRAS, 460, 2015
Sorce J. G. et al., 2016b, MNRAS, 455, 2078
Sorce J. G., 2018, MNRAS, 478, 5199
Sorce J. G., Tempel E., 2018, MNRAS, 476, 4362
Sorce J. G., Blaizot J., Dubois Y., 2019, MNRAS, 486, 3951
Tully R. B., 2015, AJ, 149, 171
Voit G. M., 2005, Rev. Mod. Phys., 77, 207
Wong A. W. C., Taylor J. E., 2012, ApJ, 757, 102
Wu H.-Y., Hahn O., Wechsler R. H., Mao Y.-Y., Behroozi P. S., 2013, ApJ, 763, 70

APPENDIX A: EXACT NUMBER OF SUBSTRUCTURES AND NEIGHBOURS OF THE SUBSAMPLES

Tables A1–A3 summarize the ranges of the number of substructures/neighbours (n) that defines each subsample as well as the number of haloes ($n_{\rm halo}$) in each one of them. For empty subsamples, the corresponding entry in the table and the line in the associated figure are absent.

Table A1. n: range of substructure numbers; $n_{\rm halo}$: number of haloes per subsample for the four panels in Fig. 3. For empty subsamples, the corresponding entry in the table and the line in the figure are absent.

Left-hand panel		Right-hand panel	
n	$n_{\rm halo}$	n	$n_{\rm halo}$
[0, 1.78]	2382		
[1.78, 3.88]	7062	0	11523
[3.88, 5.98]	6559	]0, 1.23]	6807
[5.98, 8.08]	3719		
[8.08, + ∞[	504	[1.23, + ∞[	1896
	20 226		20226

Left-hand panel		Right-hand panel	
n	$n_{\rm halo}$	n	$n_{\rm halo}$
[0, 1.55]	24		
[1.55, 4.61]	397	0	752
[4.61, 7.66]	918	]0, 1.19]	1026
[7.66, 10.7]	879	[1.19, 2.21]	614
[10.7, 13.7]	358	[2.21, 3.23]	234
[13.7, + ∞[	106	[3.23, + ∞[	56
	2682		2682

Table A3. n: range of neighbour numbers; $n_{\rm halo}$: number of haloes per subsample for the two panels in Fig. 5.

Left-hand panel		Right-hand panel	
n	$n_{\rm halo}$	n	$n_{\rm halo}$
0	4325	[0, 1.73]	377
[0, 1.16]	4703	[1.73, 3.87]	1080
[1.16, 2.28]	2671	[3.87, 6.01]	1291
[2.28, 3.40]	1113	[6.01, 8.15]	281
[3.40, + ∞[	473	[8.15, + ∞[	79
	13 285		3108

This paper has been typeset from a TEX/LATEX file prepared by the author.

Table A2. n: range of neighbour numbers; $n_{\rm halo}$: number of haloes per subsample for the 12 panels in Fig. 4.

Top left-hand panel		Top middle panel		Top right-hand panel	
n	$n_{\rm halo}$	n	$n_{\rm halo}$	n	$n_{\rm halo}$
		0	97	[0, 8.07]	145
0	4325	]0, 3.43]	3094	[8.07, 16.0]	3297
]0, 1.60]	6453	[3.43, 6.45]	7881	[16.0, 23.9]	7015
[1.60, 2.92]	4988	[6.45, 9.47]	6086	[23.9, 31.8]	6445
[2.92, 4.25]	3847	[9.47, 12.4]	2327	[31.8, 39.8]	2524
[4.25, + ∞[	613	[12.4, + ∞[	741	[39.8, + ∞[	800
	20 226		20 226		20 226

Bottom left-hand panel		Bottom middle panel		Bottom right-hand panel	
n	$n_{\rm halo}$	n	$n_{\rm halo}$	n	$n_{\rm halo}$
				[0, 1.17]	4108
0	16 926	0	8565	[1.17, 3.29]	7916
		]0, 1.85]	7212	[3.29, 5.41]	5316
]0, 1.03]	2992	[1.85, 2.81]	3149	[5.41, 7.54]	2021
[1.03, + ∞[	308	[2.81, + ∞[	1300	[7.54, + ∞[	865
	20 226		20 226		20 226

Top left-hand panel		Top middle panel		Top right-hand panel	
n	$n_{\rm halo}$	n	$n_{\rm halo}$	n	$n_{\rm halo}$
		[0, 3.71]	16	[0, 22.4]	27
[0, 1.24]	525	[3.71, 8.23]	456	[22.4, 34.6]	381
[1.24, 3.22]	1075	[8.23, 12.7]	899	[34.6, 46.8]	1003
[3.22, 5.20]	745	[12.7, 17.2]	955	[46.8, 58.9]	821
[5.20, 7.19]	257	[17.2, 21.7]	252	[58.9, 71.1]	362
[7.19, + ∞[	80	[21.7, + ∞[	104	[71.1, + ∞[	88
	2682		2682		2682

Bottom left-hand panel		Bottom middle panel		Bottom right-hand panel	
n	$n_{\rm halo}$	n	$n_{\rm halo}$	n	$n_{\rm halo}$
		0	500	[0, 3.13]	501
0	1903	]0, 1.72]	839	[3.13, 6.26]	1046
		[1.72, 3.08]	1076	[6.26, 9.39]	742
]0, 1.58]	636	[3.08, 4.44]	172	[9.39, 12.5]	282
[1.58, + ∞[	143	[4.44, + ∞[	95	[12.5, + ∞[	111
	2682		2682		2682